The Journal of Immunology

WNT-Inflammasome Signaling Mediates NOD2-Induced Development of Acute Arthritis in Mice

Vikas Singh, Sahana Holla, Subbaraya G. Ramachandra and Kithiganahalli Narayanaswamy Balaji

J Immunol 2015; 194:3351-3360; Prepublished online 25 February 2015;
doi: 10.4049/jimmunol.1402498
http://www.jimmunol.org/content/194/7/3351

The Journal of Immunology is published twice each month by
The American Association of Immunologists, Inc.,
1451 Rockville Pike, Suite 650, Rockville, MD 20852

Print ISSN: 0022-1767 Online ISSN: 1550-6606.

WNT-Inflammasome Signaling Mediates NOD2-Induced Development of Acute Arthritis in Mice

Vikas Singh,*[,1] Sahana Holla,*[,1] Subbaraya G. Ramachandra,[†] and Kithiganahalli Narayanaswamy Balaji*

In addition to its role in innate immunity, the intracellular pathogen sensor nucleotide-binding oligomerization domain 2 (NOD2) has been implicated in various inflammatory disorders, including the development of acute arthritis. However, the molecular mechanisms involved in the development of NOD2-responsive acute arthritis are not clear. In this study, we demonstrate that NOD2 signals to a cellular protein, Ly6/PLAUR domain–containing protein 6, in a receptor-interacting protein kinase 2–TGF-β–activated kinase 1–independent manner to activate the WNT signaling cascade. Gain- or loss-of-function of the WNT signaling pathway in an in vivo experimental mouse arthritis model or in vitro systems established the role for WNT-responsive X-linked inhibitor of apoptosis during the development of acute arthritis. Importantly, WNT-stimulated X-linked inhibitor of apoptosis mediates the activation of inflammasomes. The subsequent caspase-1 activation and IL-1β secretion together contribute to the phenotypic character of the inflammatory condition of acute arthritis. Thus, identification of a role for WNT-mediated inflammasome activation during NOD2 stimulation serves as a paradigm to understand NOD2-associated inflammatory disorders and develop novel therapeutics. *The Journal of Immunology*, **2015, 194: 3351–3360.**

Nucleotide-binding oligomerization domain 2 (NOD2) is an intracellular pathogen sensor that is not only effective in eliciting immune responses against the invading pathogens but also has evolved as a critical regulator of multiple inflammatory disorders (1–3). For example, allelic variants of *Nod2* were found to be associated with inflammatory bowel diseases, such as Crohn's disease (4, 5), and mutations in a single amino acid of NOD2 causes inflammatory arthritis disease, such as Blau syndrome (6–9). Although the etiology of inflammatory arthritis or acute arthritis is not very clear, they are often characterized by the presence of proinflammatory cytokines, such as IL-1β and IL-6, in the joints (7, 10). In addition to other factors, several investigations implicated the presence of bacterial cell wall components, such as peptidoglycan, in the mediation of the pathogenesis of arthritis (11, 12). Muramyl dipeptide (MDP), a component of bacterial peptidoglycan, specifically activates NOD2 signaling (1, 13). However, the identity and mechanistic details of the NOD2-triggered host pathways required for the development of arthritis are not known.

Interestingly, a few reports suggested that NOD2-responsive inflammatory disorders are caused by impairment of inflammasome functions (14, 15). Inflammasome is a multiprotein complex that activates inflammatory caspases and cytokines. During microbial or metabolic stimulation, activated inflammasome induces proteolytic activation of caspase-1 and proinflammatory IL-1β and IL-18 (14, 16, 17). However, in this regard, the molecular mediators involved in NOD2-driven inflammasome activation have not been identified.

NOD2 activates multiple signaling pathways to bring about its functions (13, 18, 19). Several investigations implicated the close association of NOD2 and the WNT signaling pathway during the development of Crohn's disease (20–22). Canonical WNT signaling involves binding of the WNT ligands to Frizzled (Fzd) and LRP5/6 coreceptors to induce stabilization of β-catenin protein. Stabilized β-catenin translocates into the nucleus to associate with the WNT-specific transcription factor, T cell factor (TCF)/lymphoid enhancer-binding factor-1 (LEF-1), and mediate the transcription of target genes. Of note, activation of WNT signaling is implicated in the development of arthritis (23–25). However, the exact mechanism of NOD2-WNT signaling cross-talk or the role for WNT signaling during inflammatory arthritis is not understood.

To unravel the molecular mechanism contributing to the development of NOD2-exacerbated arthritis, we assessed activation of the NOD2-triggered WNT pathway. Perturbation studies in both in vivo (transient mouse experimental arthritis model) and in vitro systems (using peritoneal macrophages and RAW 264.7 macrophages) emphasized the role for the NOD2-induced WNT signaling cascade in the development of acute arthritis. Importantly, we found that NOD2 activates WNT signaling in a noncanonical, receptor-interacting protein kinase 2 (RIP2)–TGF-β–activated kinase 1 (TAK1)-independent manner. NOD2 was found to complex with a positive reg-

*Department of Microbiology and Cell Biology, Indian Institute of Science, Bangalore 560012, Karnataka, India; and [†]Central Animal Facility, Indian Institute of Science, Bangalore 560012, Karnataka, India

[1]V.S. and S.H. contributed equally to this work.

Received for publication September 30, 2014. Accepted for publication January 25, 2015.

This work was supported by funds from the Department of Biotechnology and the Department of Science and Technology (under the Government of India), the Council for Scientific and Industrial Research, the Indian Council of Medical Research, and the Indo-French Center for Promotion of Advanced Research. Infrastructure support was provided by the Indian Council of Medical Research (Center for Advanced Study in Molecular Medicine), the Department of Science and Technology (Fund for Improvement of S&T Infrastructure in Universities and Higher Educational Institutions), and the University Grants Commission (special assistance to K.N.B.). V.S. was the recipient of a fellowship from the Council for Scientific and Industrial Research. S.H. was the recipient of a fellowship from the Indian Institute of Science.

Address correspondence and reprint request to Prof. Kithiganahalli Narayanaswamy Balaji, Department of Microbiology and Cell Biology, Indian Institute of Science, Bangalore 560012, Karnataka, India. E-mail address: balaji@mcbl.iisc.ernet.in

The online version of this article contains supplemental material.

Abbreviations used in this article: D/N, dominant negative; Fzd, Frizzled; LEF-1, lymphoid enhancer-binding factor-1; LYPD6, Ly6/PLAUR domain–containing protein 6; MDP, muramyl dipeptide; NLRP3, NOD-like receptor family pyrin domain–containing 3; NOD2, nucleotide-binding oligomerization domain 2; OE, overexpression; RIP2, receptor-interacting protein kinase 2; siRNA, small interfering RNA; TAK1, TGF-β–activated kinase 1; TCF, T cell factor; XIAP, X-linked inhibitor of apoptosis.

ulator of WNT signaling, Ly6/PLAUR domain–containing protein 6 (LYPD6), to stimulate and mediate WNT signaling. Exploring the functional relevance of such activation of the WNT pathway, we found that WNT induced the transcription of X-linked inhibitor of apoptosis (XIAP), which induced activation of the NOD-like receptor family pyrin domain–containing 3 (NLRP3) inflammasome complex. NOD2-stimulated formation of active caspase-1 and secretion of IL-1β were found to be dependent on WNT signaling and XIAP. Corresponding with the in vitro data, mice administered the WNT signaling inhibitor, XIAP inhibitor, or caspase-1 inhibitor exhibited a compromised ability to develop MDP-induced acute arthritis. Thus, our study provides new biological insights for the understanding of NOD2-associated inflammatory disorders.

Materials and Methods

Cells and mice

The RAW 264.7 mouse macrophage cell line was obtained from the National Center for Cell Sciences (Pune, India) and cultured in DMEM supplemented with 10% heat-inactivated FBS (both from Life Technologies), maintained at 37˚C in 5% CO_2 incubator. Primary macrophages were obtained from peritoneal exudates of C57BL/6 wild-type mice, and in vivo experiments related to the acute arthritis model were carried out in BALB/c mice. All strains of mice were purchased from The Jackson Laboratory and maintained in the Central Animal Facility, Indian Institute of Science. All studies involving mice were performed with approval of the Institutional Ethics Committee for animal experimentation, as well as from the Institutional Biosafety Committee.

Reagents and Abs

General laboratory chemicals were obtained from Sigma-Aldrich, Merck, HiMedia, or Promega. Tissue culture plasticware was purchased from Corning or Tarsons. MDP was purchased from Sigma-Aldrich. Cell culture antibiotics and anti-proliferating cell nuclear Ag Ab were obtained from Calbiochem. Anti-WNT3A, anti–Ser-33/37/Thr-41 phospho–β-catenin, anti–β-catenin, anti–Ser-9 phospho–GSK-3β, anti-RIP2, anti-TAK1, anti–IL-1β, anti–caspase-1, anti-XIAP, and anti-NLRP3 Abs were obtained from Cell Signaling Technology. PE-conjugated F4/80 was purchased from Tonbo Biosciences. Anti–β-actin Ab and DAPI were purchased from Sigma-Aldrich. HRP-conjugated and DyLight 488–conjugated anti-rabbit/mouse IgG Abs and HRP-conjugated streptavidin were purchased from

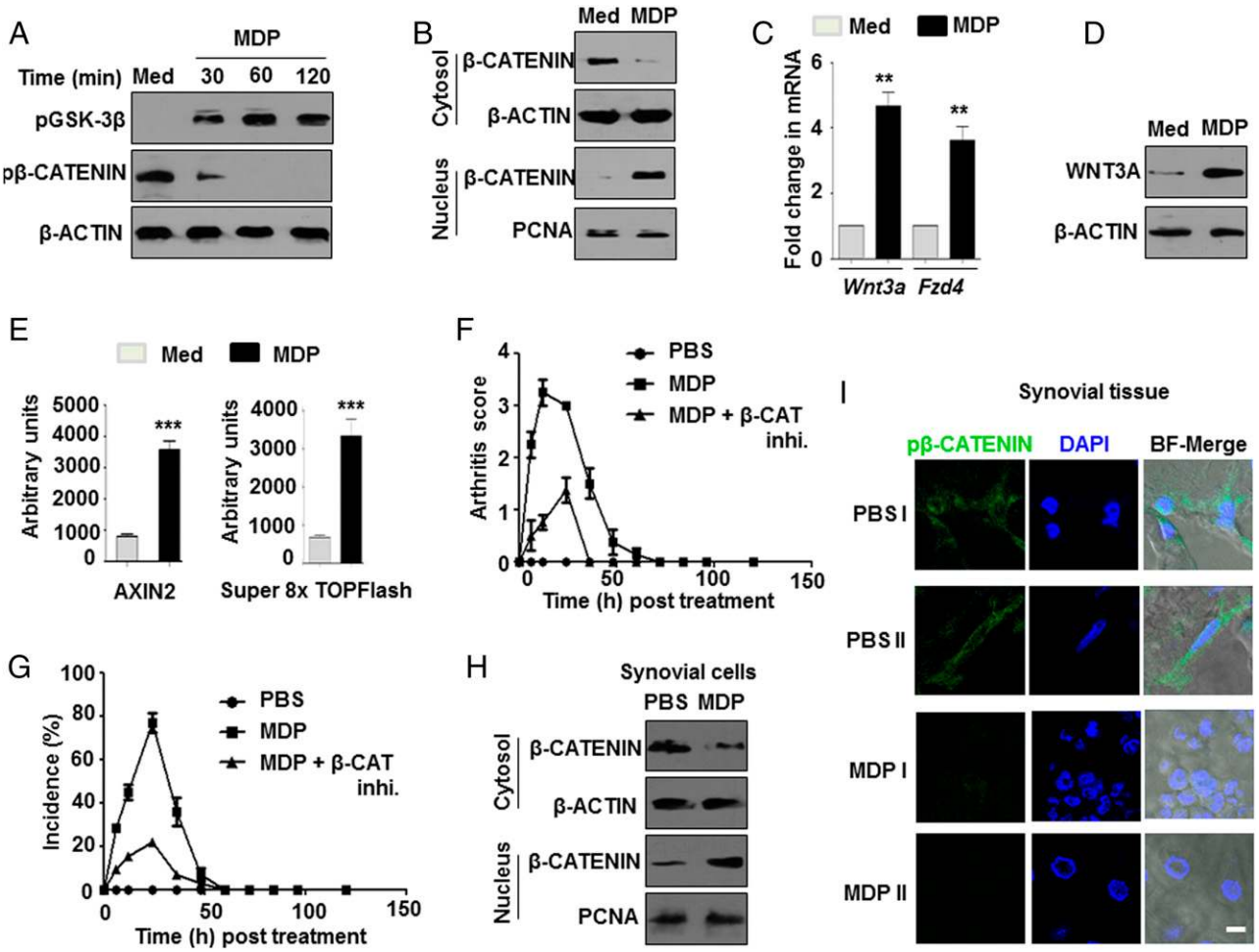

FIGURE 1. NOD2-activated WNT signaling is required for development of acute arthritis. Mouse peritoneal macrophages were treated with MDP (a NOD2 agonist) for the indicated times, and phosphorylation of GSK-3β and β-catenin (**A**) and translocation of β-catenin from cytosol to nucleus (**B**) were analyzed by immunoblotting. *Wnt3a* and *Fzd4* transcripts (**C**) and WNT3A protein expression (**D**) were assessed by quantitative real-time RT-PCR and immunoblotting, respectively. (**E**) RAW 264.7 macrophages were transfected with AXIN2 (*left panel*) or Super 8x TOPFlash (*right panel*) luciferase construct, followed by MDP treatment for 12 h. Promoter activity was measured by a luciferase reporter assay. (**F** and **G**) Mice were challenged i.v. with β-catenin inhibitor (β-CAT inhi.) (50 mg/kg bodyweight) for 2 h prior to MDP (100 μg/mice) injection. Arthritis score (F) and incidence of arthritis (G) in each of the above-mentioned cases for given time points was assessed by the *t* test and χ^2 test, respectively. (**H**) Synovial cells were isolated from mice that were challenged i.v. with PBS or MDP for 24 h. β-catenin translocation to nucleus was analyzed by immunoblotting. (**I**) Representative immunofluorescence images of phosphorylated β-catenin in the cryosections of the synovial tissues isolated from mice challenged with PBS or MDP (n = 4/group). Scale bar, 5 μm. The immunoblotting data shown are representative of results obtained from three independent experiments. Quantitative real-time RT-PCR data and luciferase assay data represent the mean ± SEM for three independent experiments. $^{**}p < 0.005$, one-way ANOVA. $^{***}p < 0.0001$, *t* test. Med, medium; PCNA, proliferating cell nuclear Ag.

Jackson ImmunoResearch. Anti-NOD2 Ab was obtained from Santa Cruz Biotechnology, and anti-GFP Ab was obtained from Invitrogen.

Plasmids and constructs

Super 8x TOPFlash and AXIN2 reporter constructs were purchased from Addgene. NOD2 cDNA and RIP2 dominant-negative (D/N) constructs were generous gifts from Dr. Derek W. Abbott (Case Western Reserve University School of Medicine, Cleveland, OH). The TAK1 D/N construct was obtained from Dr. Jun Nonomiya-Tsuji (North Carolina State University, Raleigh, NC). XIAP overexpression (OE) and XIAP D/N constructs were kind research gifts from Dr. Jonathan D. Ashwell (National Cancer Institute, National Institutes of Health, Bethesda, MD). spGFP-LYPD6 cDNA and spGFP-LYPD6 D/N constructs were gifted by Dr. Gilbert Weidinger (Institute for Biochemistry and Molecular Biology, Ulm University, Ulm, Germany). TCF4 D/N construct was obtained from Dr. Roel Nusse (Stanford University Medical Center, Stanford, CA). β-galactosidase reporter construct was a generous research gift from Dr. Kumaravel Somasundaram (Indian Institute of Science).

Treatment with pharmacological reagents in vitro

Cells were treated with the following inhibitors 1 h prior to the experimental treatments: β-catenin inhibitor (15 μM; Calbiochem); PP2 (500 nM; Calbiochem), and Embelin (10 μM; Sigma-Aldrich). DMSO (0.1%) was used as the vehicle control. In all experiments involving pharmacological reagents, a tested concentration was used after careful titration experiments assessing the viability of the macrophages using the MTT (3-(4,5-Dimethylthiazol-2-yl)-2,5-diphenyltetrazolium bromide) assay.

Transfection studies

Murine RAW 264.7 macrophages were transiently transfected with the indicated plasmids (D/N or OE or luciferase constructs) using low m.w. polyethylenimine. In experiments involving small interfering RNA (siRNA), RAW 264.7 macrophages were transfected with 100 nM siRNA against *Card15*, *Ripk2*, *Map3k7*, *β-Catenin*, or *Xiap*, nontargeting siRNA, or siGLO Lamin A/C, which were obtained from Dharmacon as siGENOME SMARTpool reagents, which contain a pool of four dsRNA oligonucleotides. Transfection efficiency was >50% in all experiments, as determined by counting the number of siGLO Lamin A/C$^+$ cells in a microscopic field using a fluorescent microscope. In all cases, the cells were treated as indicated 48 h postinfection and processed for analysis.

Luciferase assay

Treated cells were lysed in Reporter Lysis Buffer and assayed for luciferase activity using Luciferase Assay Reagent (both from Promega), as per the manufacturer's instructions. The results were normalized with transfection efficiency measured by galactosidase activity. *O*-nitrophenol β-D-galactopyranoside (HiMedia) was used as substrate for the galactosidase assay.

RNA isolation and quantitative real-time RT-PCR

Macrophages were treated as indicated, and total RNA from macrophages was isolated by TRI Reagent (Sigma-Aldrich). A total of 1.5 μg total RNA was converted into cDNA using a First-Strand cDNA synthesis kit (Bioline). Quantitative real-time RT-PCR was performed using SYBR Green PCR

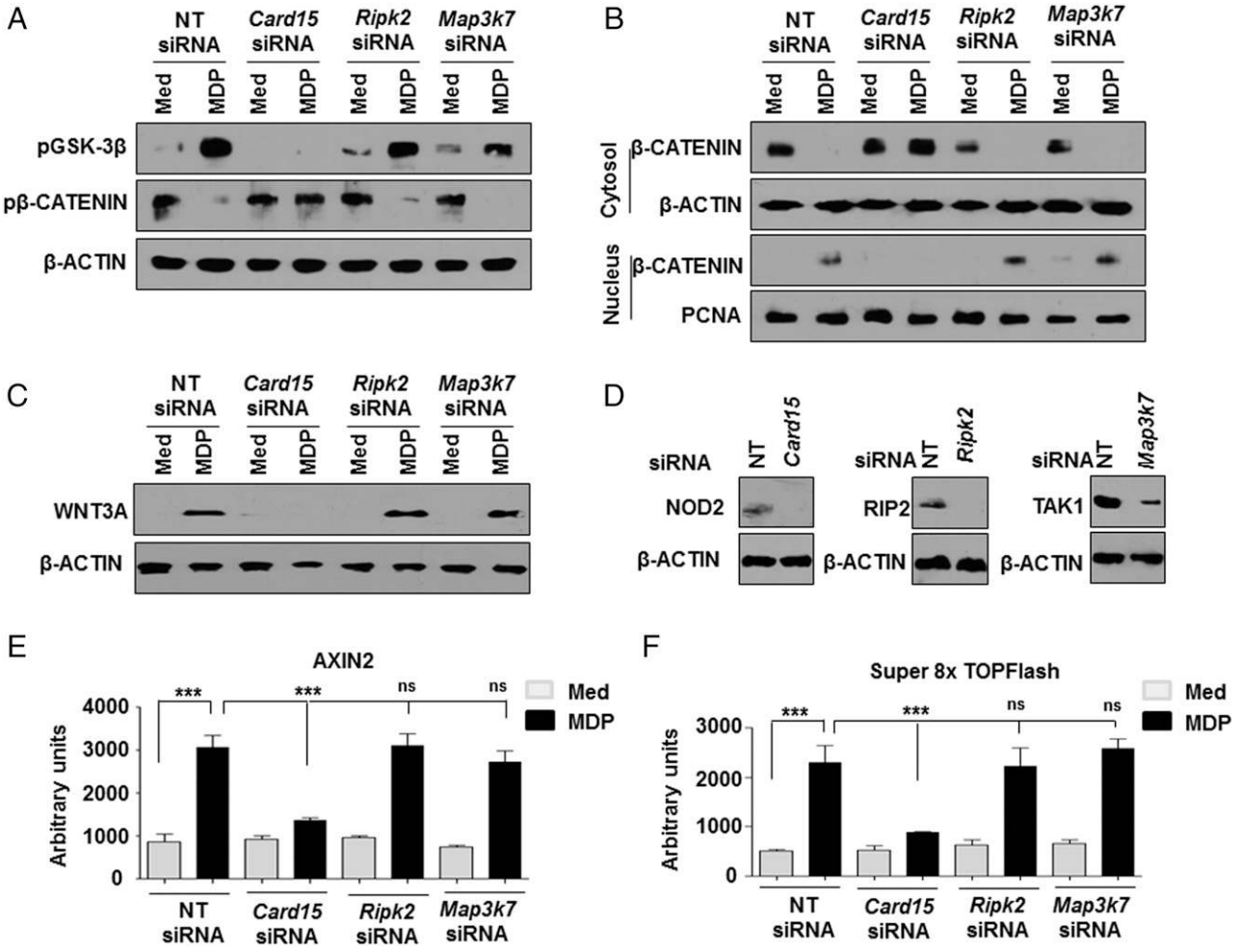

FIGURE 2. NOD2-induced WNT signaling activation is independent of the RIP2–TAK1 axis. (**A**–**C**) RAW 264.7 macrophages were transfected with *Card15*-, *Ripk2*-, or *Map3k7*-specific siRNA, followed by MDP treatment. Phosphorylation status of GSK-3β and β-catenin (A), the expression of β-catenin in cytosolic and nuclear fractions (B), and WNT3A (C) were analyzed by immunoblotting. (**D**) Validation of *Card15*-, *Ripk2*-, and *Map3k7*-specific siRNAs. RAW 264.7 macrophages were cotransfected with *Card15*-, *Ripk2*-, or *Map3k7*-specific siRNA with AXIN2 (**E**) or Super 8x TOPFlash (**F**) luciferase construct, followed by MDP treatment for 12 h. Promoter activity was measured by a luciferase reporter assay. The immunoblotting data are representative of three independent experiments. Luciferase assay data represent the mean ± SEM for three independent experiments. ***$p < 0.0001$, one-way ANOVA. Med, medium; ns, not significant; NT, nontargeting; PCNA, proliferating cell nuclear Ag.

mixture (KAPA Biosystems) for quantification of the target gene expression. All of the experiments were repeated at least three times independently to ensure reproducibility of the results. *Gapdh* was used as internal control. The primers used for quantitative real-time RT-PCR amplification were as follow: *Gapdh* forward 5′-GAGCCAAACGGGTCATCATCT-3′, reverse 5′-GAGGGGCCATCCACAGTCTT-3′; *Wnt3a* forward 5′-TGGCTGAGGGTGTCAAAGC-3′, reverse 5′-CGTGTCACTGCGAAAGCTACT-3′; *Fzd4* forward 5′-AACCTCGGCTACAACGTGAC-3′, reverse 5′-TTGGCACATAAACCGAACAA-3′; *IL-1β* forward 5′-GAAATGCCACCTTTTGACAGTG-3′, reverse 5′-TGGATGCTCTCATCAGGACAG-3′; and *Xiap* forward 5′-CGAGCTGGGTTTCTTTATACCG-3′, reverse 5′-GCAATTTGGGGATATTCTCCTGT-3′.

Cell lysate preparation and Western blot analysis

Treated cells were pelleted and lysed in RIPA buffer (50 mM Tris-HCl [pH 7.4]; 1% Nonidet P-40; 0.25% sodium deoxycholate; 150 mM NaCl; 1 mM EDTA; 1 mM PMSF; 1 μg/ml each aprotinin, leupeptin, and pepstatin; 1 mM Na_3VO_4; 1 mM NaF) on ice for 30 min. Whole-cell lysates were collected. An equal amount of protein from each cell lysate was subjected to SDS-PAGE and transferred onto polyvinylidene difluoride membranes (Millipore) by a semidry Western blotting method (Bio-Rad). Nonspecific binding was blocked with 5% nonfat dry milk powder in TBST (20 mM Tris-HCl [pH 7.4], 137 mM NaCl, and 0.1% Tween 20) for 60 min. The blots were incubated overnight at 4˚C with primary Ab diluted in TBST with 5% BSA. After washing with TBST, blots were incubated for 2 h with anti-rabbit or anti-mouse IgG secondary Abs conjugated to HRP. The immunoblots were developed with an ECL detection system (PerkinElmer), per the manufacturer's instructions. β-actin was used as loading control.

Nuclear and cytosolic subcellular fractionation

Harvested cells were gently resuspended in ice-cold Buffer A (10 mM HEPES [pH 7.9], 10 mM KCl, 0.1 mM EDTA, 0.1 mM EGTA, 1 mM DTT, and 0.5 mM PMSF). After incubation on ice for 15 min, cell membranes were disrupted with 10% Nonidet P-40, and the nuclear pellets were obtained after centrifugation at 13,000 rpm for 15 min at 4˚C. The supernatants from this step were used as cytosolic extracts. Nuclear pellets were lysed with ice-cold Buffer C (20 mM HEPES [pH 7.9], 0.4 M NaCl, 1 mM EDTA, 1 mM EGTA, 1 mM DTT, and 1 mM PMSF), and nuclear extracts were collected. An equal amount of protein from each cell lysate was subjected to SDS-PAGE. β-actin was used as a loading control for the cytosolic fraction and anti-proliferating cell nuclear Ag was used for the nuclear fraction.

Immunoprecipitation assay

Immunoprecipitation assays were performed using a protocol provided by Millipore, with certain modifications. Briefly, macrophages were gently lysed in ice-cold RIPA buffer on an orbital shaker. The cell lysates were incubated with anti-GFP, anti-NLRP3, or rabbit preimmune sera at 4˚C for 2 h on an orbital shaker. The immune complexes were captured using Protein A (Bangalore Genei) agarose at 4˚C for 2 h. The beads were harvested, washed, and boiled in 5× Laemmli buffer for 10 min. The samples were subjected to immunoblotting.

Enzyme immunoassay (ELISA)

Measurement of IL-1β levels in the cell-free culture supernatants was carried out using an IL-1β ELISA kit (BD Biosciences), following the manufacturer's instructions. Briefly, assay plates were coated with anti–IL-1β capture Abs overnight at 4˚C, followed by incubation with 1% BSA for 1 h at room temperature. After three washes with PBST (1× PBS with 0.05% Tween 20), plates were incubated with cell-free culture supernatants for 2 h, followed by incubation with anti–IL-1β detection Abs for 2 h at room temperature. After further incubation of plates with streptavidin-HRP Abs for 1 h at room temperature, reactions were developed with 3,3′,5,5′-tetramethylbenzidine. The absorbance was measured in an ELISA reader (Molecular Devices) at 450 nm.

Experimental acute arthritis model

MDP-induced experimental acute arthritis was developed in BALB/c mice, as previously described (6). All of the studies related to the experimental acute arthritis model were performed under the supervision of S.G.R., Principal Research Scientist and a qualified Veterinarian of the Central Animal Facility, Indian Institute of Science. Other than the phenotypic characteristics of MDP-induced acute arthritis, the health status of all mice used in the study was normal. Neither of the inhibitors used in the current study caused any other visible effects, such as weight loss or health problems, in the mice. Briefly, mice were injected i.v. or

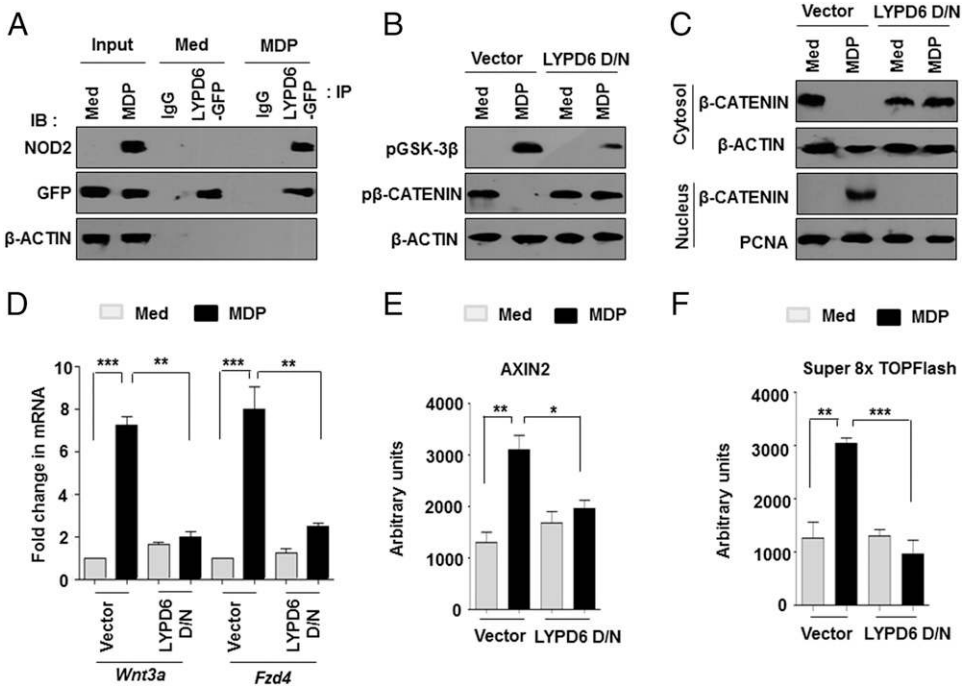

FIGURE 3. LYPD6 mediates NOD2-triggered WNT signaling activation. (**A**) Anti-GFP immunoprecipitation (IP) was performed with GFP-LYPD6–transfected RAW 264.7 macrophages that were treated with MDP for 1 h. The immunoprecipitates were subjected to immunoblotting (IB) using the indicated Abs. (**B**–**F**) RAW 264.7 macrophages were transfected with LYPD6 D/N, as indicated. At 48 h posttransfection, cells were treated with MDP for 1 h (B and C) or 12 h (D–F). WNT signaling activation markers (B–D) were analyzed by IB and quantitative real-time RT-PCR, or AXIN2 (E) and Super 8x TOPFlash (F) luciferase assays were performed. IB data are representative of results obtained from three independent experiments. Quantitative real-time RT-PCR data and luciferase data represent the mean ± SEM for three independent experiments. $*p < 0.05$, $**p < 0.005$, $***p < 0.0001$, one-way ANOVA. Med, medium; PCNA, proliferating cell nuclear Ag.

not with pharmacological inhibitors (β-catenin inhibitor [50 mg/kg bodyweight], Embelin [10 mg/kg bodyweight], or caspase-1 inhibitor [50 mg/kg bodyweight] [Calbiochem]) for 2 h prior to i.v. challenge with MDP (100 μg/mice). Control mice received sterile PBS. Each experimental group contained six mice. The treated mice were used for either scoring or for biochemical analysis. The development of arthritis in the hind ankles and feet was evaluated for each paw. The arthritis score is the sum of the inflammation scores for both hind paws, which were graded on a scale from 0 to 4: 0, normal paw with no redness or swelling; 1, some swelling of ankle; 2, moderate swelling and redness of ankle; 3, moderate swelling and redness of ankle along with some swelling of foot pad and/or digits; and 4, pronounced swelling and redness of the entire paw. Incidence of arthritis represents the percentage of mice whose arthritis score was ≥1. Data for arthritis score and incidence were assessed by the *t* test and χ^2 test, respectively. Cells from hind leg paws and synovium were subjected to total RNA isolation and immunoblotting for biochemical analysis. Cryosections of the synovial tissues were used for immunohistochemistry.

Synovial cell isolation

Synovial cells from mice were isolated, as previously described, with certain modifications (26). Briefly, mice were positioned such that the knee joints were exposed by a midline skin incision. Transverse resection of the quadriceps at the middle followed by distally reversing the tissue exposed the synovium, patella, and patellar ligament. Synovial tissues were then resected and treated with filtered collagenase IV (1 mg/ml; HiMedia) containing DMEM with 10% FBS at 37°C for 60 min. Samples were vortexed vigorously, and the resultant supernatant was collected to separate the tissue debris. The collected samples were further centrifuged at 1500 rpm for 10 min at 4°C. Pelleted cells were resuspended in fresh DMEM supplemented with 10% FBS and seeded for 2 h. Adherent cells were harvested as macrophages and used for immunoblotting.

Cryosectioning of the synovial tissues

The excised synovial tissues (mentioned earlier) were rapidly frozen in liquid nitrogen in OCT medium (Jung; Leica). Cryosections (15 μm) were taken with the tissue embedded in OCT on the glass slides and stored at −80°C.

Immunofluorescence

The frozen tissue sections were thawed to room temperature, fixed with 4% paraformaldehyde, and washed with PBS. After blocking with 2% BSA containing saponin, the sections were stained for specific Abs at 4°C overnight. The sections were incubated with DyLight 488–conjugated secondary Ab for 2 h, and nuclei were stained with DAPI for 2 min. A coverslip was mounted on the section with glycerol as the medium. Confocal images were taken using a Zeiss LSM 710 Meta confocal laser scanning microscope using a Plan-Achromat 63×/1.4 Oil DIC objective (both from Carl Zeiss), and images were analyzed using ZEN 2009 software.

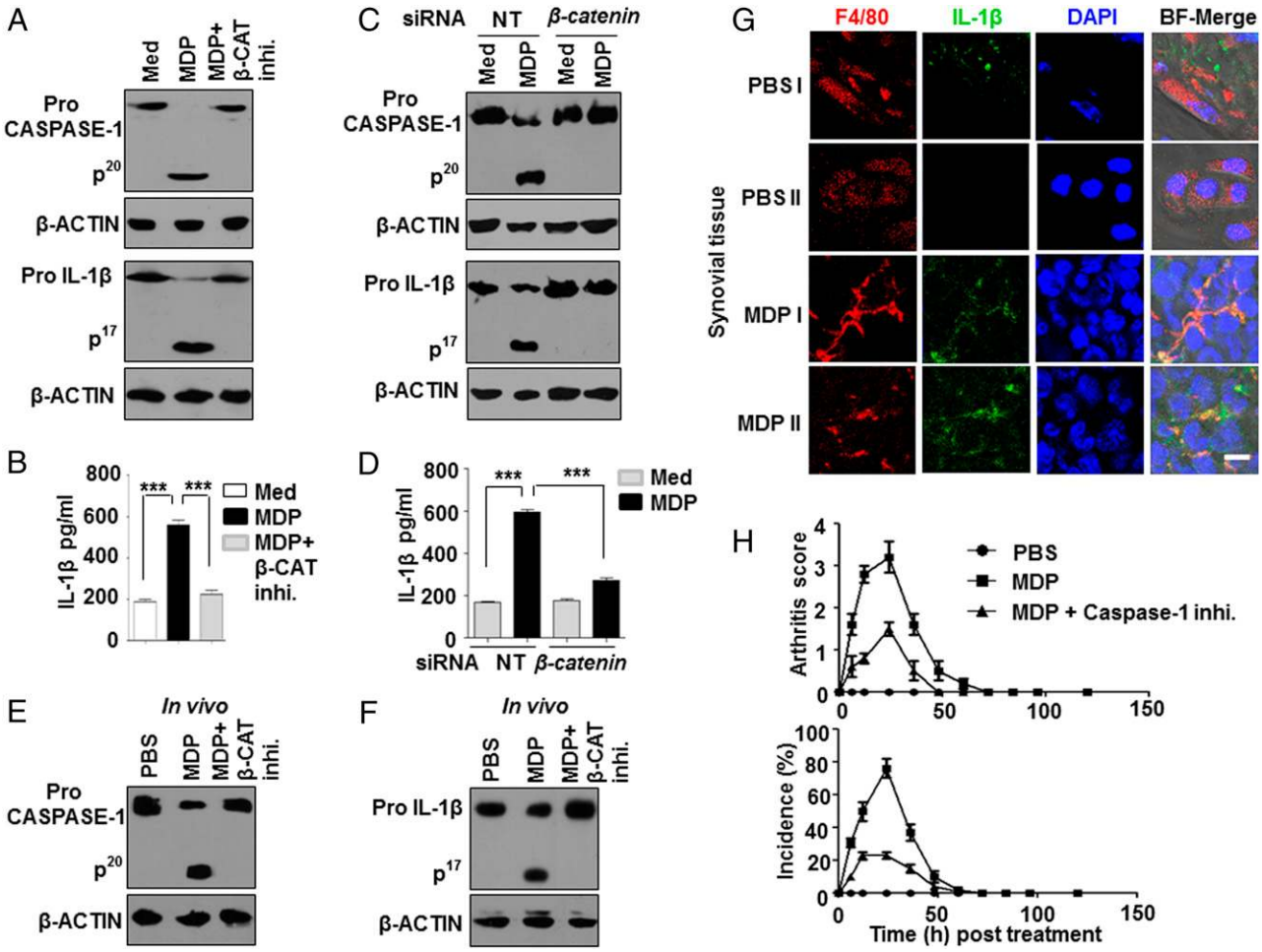

FIGURE 4. WNT signaling is essential for NOD2-dependent inflammasome activation. Macrophages pretreated with β-catenin inhibitor (β-CAT inhi.) (**A** and **B**) or RAW 264.7 macrophages transfected with *β-catenin* siRNA (**C** and **D**) were treated with MDP and assessed for activated caspase-1 and IL-1β by immunoblotting (A and C) and secretion of IL-1β by ELISA (B and D). (**E** and **F**) Mice were challenged i.v. with β-CAT inhi. (50 mg/kg bodyweight) for 2 h prior to MDP (100 μg/mice) injection for 12 h. Activated caspase-1 (E) and IL-1β (F) were assessed by immunoblotting cells obtained from hind paws. (**G**) Representative immunofluorescence images of cryosections of the synovial tissues isolated from mice challenged with PBS or MDP (n = 4/group) and stained for F4/80 (PE conjugated), IL-1β (DyLight 488), and DAPI. Scale bar, 5 μm. (**H**) Mice were challenged i.v. with caspase-1 inhibitor (50 mg/kg bodyweight) for 2 h prior to MDP injection. Arthritis score (*upper panel*) and incidence of arthritis (*lower panel*) were assessed by the *t* test and χ^2 test, respectively. Immunoblotting data are representative of results obtained from three independent experiments. ELISA data represent the mean ± SEM of three independent experiments. ***$p < 0.0001$, one-way ANOVA. Med, medium; NT, nontargeting.

Statistical analysis

Levels of significance for comparison between samples were determined by the Student *t* test and one-way ANOVA. Data in the graphs are expressed as mean ± SE for five or six values from three independent experiments, and p values < 0.05 were defined as significant. GraphPad Prism 5.0 software (GraphPad) was used for all statistical analyses.

Results

WNT signaling regulates development of NOD2-induced acute arthritis

NOD2 and WNT signaling have been independently ascribed to mediate the pathogenesis of arthritis (6, 24). To explore the role for WNT signaling during NOD2-induced development of arthritis, activation of the WNT cascade was assessed in macrophages treated with a specific NOD2 ligand, MDP. The phosphorylation status of β-catenin and GSK-3β (Fig. 1A), nuclear translocation of total β-catenin (Fig. 1B), transcript levels of WNT-responsive genes *Wnt3a* and *Fzd4* (Fig. 1C), and protein expression of WNT3A (Fig. 1D) suggested NOD2-induced activation of the canonical WNT pathway. Phosphorylated β-catenin (Ser^{33}, Ser^{37}, Thr^{41}) indicates inactivation of the WNT pathway and Ser^{9} phosphorylation of GSK-3β suggests activated WNT signaling. Supporting this observation, activation of NOD2 signaling also showed increased AXIN2 (a WNT-responsive gene) promoter activity (Fig. 1E, *left panel*) and TCF/LEF-dependent promoter activity (Fig. 1E, *right panel*). These results suggest NOD2-responsive activation of WNT signaling. Further, to validate the results obtained from in vitro experiments, an in vivo model of transient acute arthritis was developed in BALB/c mice following i.v. injection of MDP (6). As assessed using the arthritis score and incidence of arthritis, MDP-treated mice showed an enhanced phenotype of acute arthritis that was significantly abrogated in the presence of a pharmacological inhibitor of β-catenin (Fig. 1F, 1G). Corroborating this, cells from the synovial tissue of MDP-treated mice displayed activated WNT signaling, as seen by nuclear translocation of total β-catenin (Fig. 1H) and reduced phosphorylated β-catenin (Fig. 1I). These results indicate a crucial role for WNT signaling in regulating NOD2-induced acute arthritis in mice.

RIP2–TAK1 axis is dispensable for NOD2-triggered WNT signaling activation

Classically, NOD2 activation leads to the recruitment of the cytosolic adaptor proteins RIP2 and TAK1, which, in turn, activate the downstream cascade (1). To assess the possible roles for RIP2 and TAK1 in the current study, RNA interference of *Card15* (NOD2), *Ripk2* (RIP2), and *Map3k7* (TAK1) was carried out. Interestingly, although NOD2-specific siRNA-transfected macrophages failed to activate the MDP-induced WNT signaling pathway (Fig. 2), RIP2- or TAK1-specific siRNA (Fig. 2) or D/N construct (Supplemental Fig. 1) transfected cells did not show such effects. These observations underscore the NOD2-dependent, RIP2-TAK1–independent activation of WNT signaling in the current scenario.

LYPD6 is essential to activate WNT signaling by NOD2

Having established that NOD2-mediated WNT signaling activation was independent of the RIP2–TAK1 axis, the role for another potential mediator of the pathway, LYPD6, was assessed. Recently, LYPD6 was found to recruit to the WNT receptor complex to positively regulate WNT signaling (27, 28). Interestingly, MDP-induced membrane recruitment of NOD2 to activate downstream signaling is well established (29, 30). Thus, we explored the possible role for NOD2-LYPD6–mediated WNT activation. Coimmunoprecipitation experiments confirmed NOD2–LYPD6 regulatory interactions during MDP stimulation (Fig. 3A). Further, although inhibition of LYPD6 activity in macrophages severely

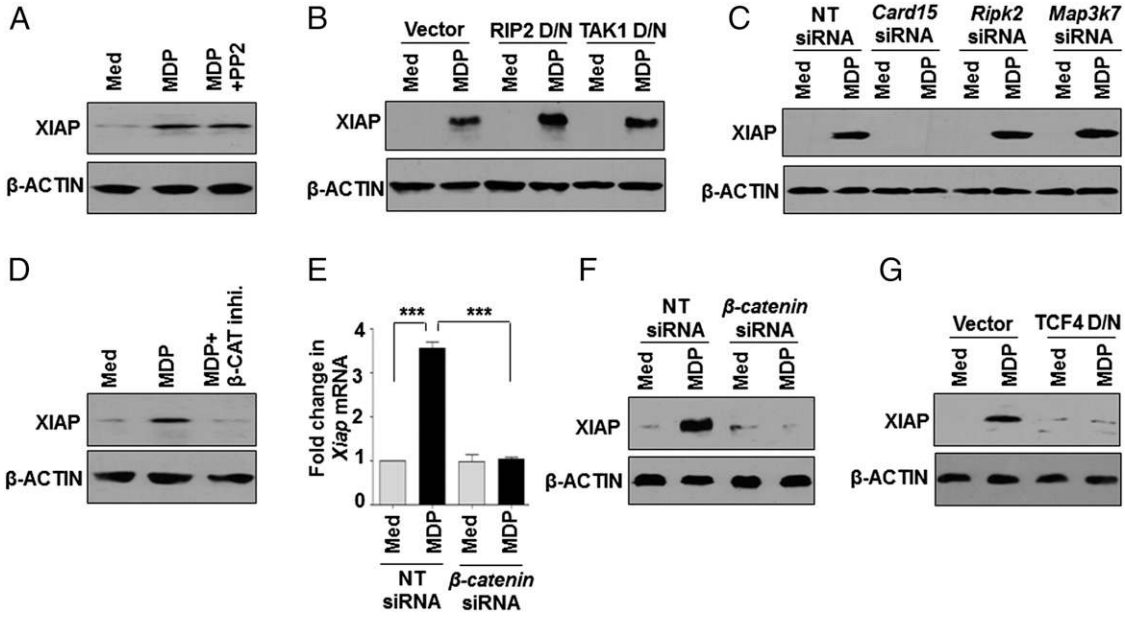

FIGURE 5. RIP2/TAK1-independent expression of NOD2-WNT–responsive XIAP. (**A**) Mouse peritoneal macrophages were treated with PP2 (RIP2 inhibitor) for 1 h prior to a 12-h MDP treatment (100 ng), and expression of XIAP was analyzed by immunoblotting. RAW 264.7 macrophages were transfected with RIP2 or TAK1 D/N (**B**) or *Card15*-, *Ripk2*-, or *Map3k7*-specific siRNA (**C**), and expression of XIAP was assessed by immunoblotting. (**D**) Mouse peritoneal macrophages were treated with β-catenin inhibitor (β-CAT inhi.) for 1 h prior to MDP treatment for 12 h, and expression of XIAP was analyzed by immunoblotting. RAW 264.7 macrophages were transfected with *β-catenin*–specific siRNA (**E** and **F**) or a TCF4 D/N construct (**G**), followed by MDP treatment. The transcript level of *Xiap* (E) and the protein level of XIAP (F and G) were determined by quantitative real-time RT-PCR and immunoblotting, respectively. The immunoblotting data are representative of results obtained from three independent experiments. Quantitative real-time RT-PCR data represent the mean ± SEM of three independent experiments. ***$p < 0.0001$, one-way ANOVA. Med, medium; NT, nontargeting.

hindered the ability of NOD2 to activate WNT signaling (Fig. 3B–F), OE of LYPD6 was sufficient to activate the WNT signaling pathway (Supplemental Fig. 2).

WNT signaling mediates NOD2-induced inflammasome activation

Further, we investigated the functional role of LYPD6-mediated activation of WNT signaling in arbitrating NOD2-responsive inflammatory arthritis. Induction of NOD2 signaling is often associated with activation of NLRP3/NALP3/Cryopyrin inflammasome, marked by the maturation of proinflammatory cytokines (17, 31). Thus, a role for WNT signaling, if any, during NOD2-induced inflammasome activation was assessed. Inflammasome activation was analyzed by cleavage of caspase-1 and IL-1β from their pro forms to activated p^{20} and p^{17} products, respectively, as well as by estimating *Il-1β* mRNA expression and secreted levels of active IL-1β. Interestingly, although MDP-stimulated macrophages displayed robust activation of inflammasomes, macrophages pretreated with β-catenin inhibitor (WNT signaling inhibitor) (Fig. 4A, 4B, Supplemental Fig. 3A) or transfected with *β-catenin* siRNA (Fig. 4C, 4D, Supplemental Fig. 3B, 3C) exhibited compromised activation of inflammasomes by NOD2. Notably, corroborating these in vitro observations, WNT signaling–dependent activation of inflammasome was found in the cells from hind leg paws of mice with acute arthritis (Fig. 4E, 4F, Supplemental Fig. 3D), and macrophages were found to be the source of most of the IL-1β in the synovial tissue (Fig. 4G). Next, the role of inflammasome activation in the development of NOD2-induced acute arthritis was confirmed using caspase-1 inhibitor. MDP-treated mice displayed an enhanced phenotype of acute arthritis that was significantly abrogated in mice pretreated with caspase-1 inhibitor (Fig. 4H).

NOD2-activated inflammasomes are XIAP dependent

To further delineate the mechanism of WNT-mediated activation of NOD2-dependent inflammasomes, we analyzed the contribution of XIAP. XIAP is a known WNT-responsive gene (32, 33) and is implicated during innate immune cytokine responses (34), making it a suitable regulator candidate. In line with the previous observations (Fig. 2), the macrophages pretreated with RIP2 pharmacological inhibitor (Fig. 5A) or transfected with D/N forms (Fig. 5B) or specific siRNAs (Fig. 5C) of RIP2 or TAK1 did not exhibit any change in MDP-induced XIAP expression. This suggests that induced expression of XIAP is NOD2 dependent but is independent of RIP2 or TAK1 signaling. Further, pharmacological inhibition (Fig. 5D) or RNA-mediated interference (Fig. 5E, 5F) of β-catenin in macro-

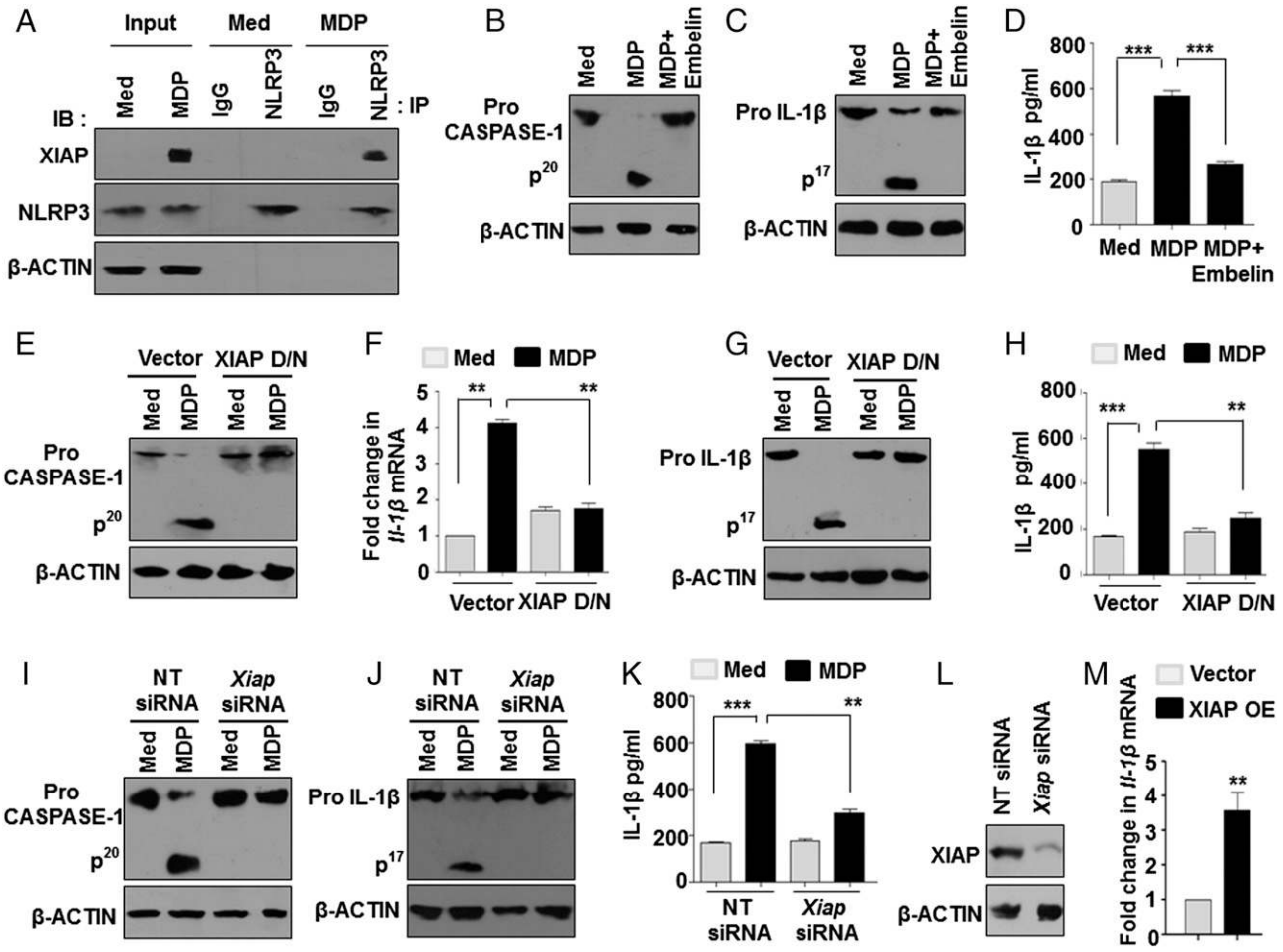

FIGURE 6. XIAP is required for NOD2-dependent inflammasome activation. (**A**) Anti-NLRP3 immunoprecipitation (IP) was performed with peritoneal macrophages treated with MDP for 12 h. The immunoprecipitates were subjected to immunoblotting (IB) using the indicated Abs. Peritoneal macrophages pretreated with Embelin (XIAP inhibitor) (**B**–**D**) and XIAP D/N–transfected (**E**–**H**) or *Xiap* siRNA–transfected (**I**–**L**) or XIAP OE–transfected (**M**) RAW 264.7 macrophages were treated with MDP, as indicated, and assessed for inflammasome markers, caspase-1, and IL-1β by IB, quantitative real-time RT-PCR, and ELISA. IB data are representative of results obtained from three independent experiments. ELISA and quantitative real-time RT-PCR data represent the mean ± SEM of three independent experiments. $^{**}p < 0.005$, $^{***}p < 0.0001$, one-way ANOVA. *t* test in (M). Med, medium; NT, nontargeting.

phages or experiments using TCF4 D/N constructs (Fig. 5G) validated that NOD2-induced expression of XIAP was arbitrated by WNT signaling.

Importantly, in line with the previous reports of NOD2 signaling–stimulated NLRP3 inflammasome (17, 31), MDP stimulation of macrophages induced the association of XIAP with NLRP3 (Fig. 6A). Importantly, we found an essential role for XIAP during NOD2-directed inflammasome activation because MDP-induced cleavage of caspase-1 and IL-1β or expression and secretion of IL-1β was severely compromised in macrophages treated with the pharmacological inhibitor of XIAP, Embelin (Fig. 6B–D), or transfected with the XIAP D/N construct (Fig. 6E–H) or *Xiap*-specific siRNA (Fig. 6I–L). Corresponding with these data, XIAP OE in the macrophages induced increased expression of *Il-1β* (Fig. 6M).

XIAP is an essential link in NOD2-driven induction of acute arthritis in mice

Supporting the in vitro experiments, cells from mice that were treated i.v. with Embelin prior to MDP challenge displayed reduced activation of inflammasomes compared with the mice that were challenged with MDP alone, as assessed by the expression of *Il-1β* (Fig. 7A) and cleavage of caspase-1 and IL-1β (Fig. 7B, 7C). Notably, Embelin-treated mice showed compromised characteristics of development of MDP-orchestrated acute arthritis, as assessed by the arthritis score (Fig. 7D) and incidence (Fig. 7E). These results indicate that, upon MDP treatment and NOD2 activation, WNT-induced XIAP expression mediates inflammasome activation to cause acute arthritis in mice (Fig. 7F).

Discussion

NOD2 signaling is strongly implicated in the exacerbation of several inflammatory disorders, including arthritis. In fact, detectable levels of bacterial cell wall components like peptidoglycans, MDP, and increased expression of NOD2 were found in the synovial fluid of the joints of rheumatoid arthritis patients (11, 12, 35). Although investigations were carried out to understand the functions of NOD2 signaling in several arthritis models (6, 7, 11), the mechanism of induction of local joint inflammation by NOD2 signaling is not clear.

Of note, macrophages are known to critically regulate the pathogenesis of rheumatoid arthritis (36). With NOD2 being an established pattern recognition receptor that is abundant in macrophages (37), we first sought to determine the mechanistic details of induced NOD2 signaling in macrophages and, subsequently, in inflammatory joints, using the well-established experimental acute arthritis model of mice (6). Importantly, the macrophages in the synovial tissues of MDP-treated mice secreted IL-1β, a signature cytokine that directs acute arthritis. Both in vitro and in vivo experiments suggested that development of NOD2-mediated acute arthritis was WNT signaling dependent. Although probable NOD2–WNT cross-talk (20) or an important role for WNT signaling during development of rheumatoid arthritis (23) was

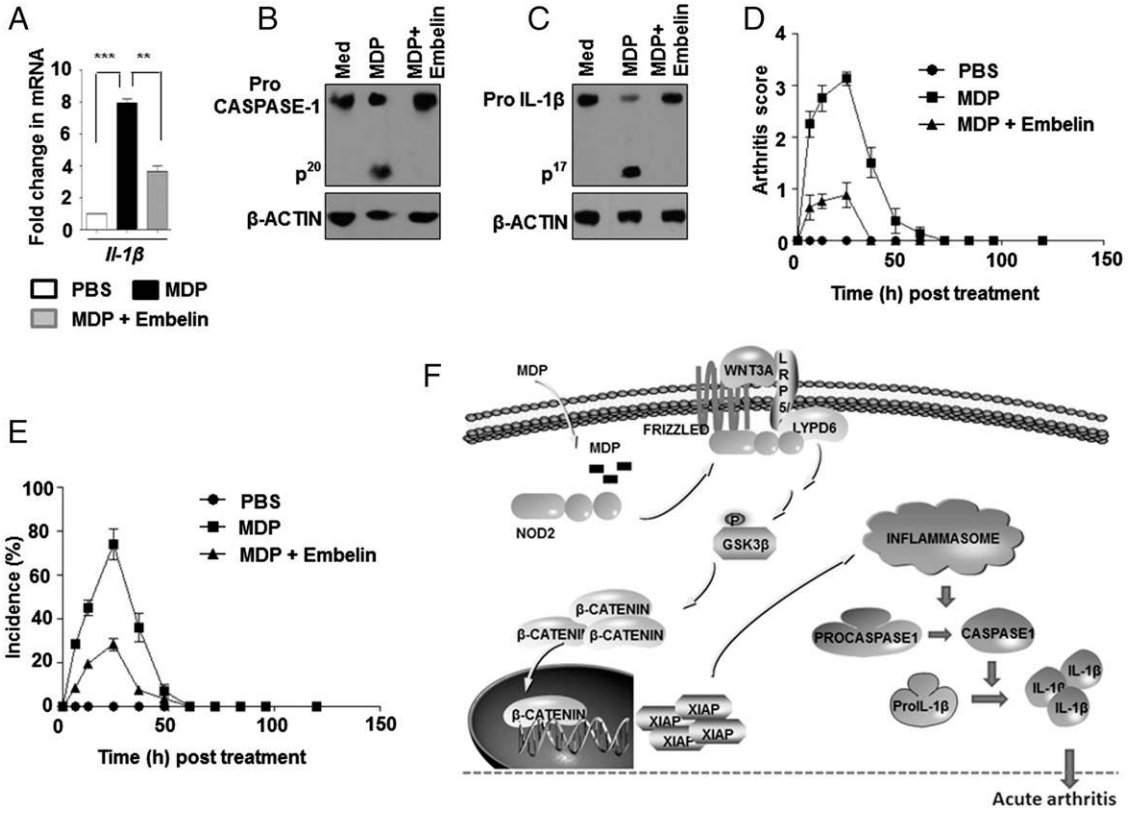

FIGURE 7. XIAP plays a critical role during development of NOD2-triggered acute arthritis in mice. (**A**–**C**) Mice were challenged i.v. with Embelin (10 mg/kg bodyweight) for 2 h prior to MDP (100 μg/mice) injection for 12 h. mRNA level of *Il-1β* (A) and the active form of caspase-1 (B) and IL-1β (C) were analyzed by quantitative real-time RT-PCR (A) or immunoblotting (B and C) from the cells obtained from mice hind paws. Arthritis score (**D**) and incidence of arthritis (**E**) in each of the above-mentioned cases was assessed by the *t* test and χ^2 test, respectively. (**F**) Proposed model for the mechanism involved in NOD2-induced acute arthritis. NOD2 signals to a cellular protein, LYPD6, in a RIP2-TAK1–independent manner to activate the WNT signaling cascade. Perturbation of the NOD2-induced WNT signaling pathway leads to compromised expression of XIAP, which is required for the development of acute arthritis. Importantly, WNT-stimulated XIAP mediates activation of the inflammasome. Immunoblotting data are representative of results obtained from three independent experiments. Quantitative real-time RT-PCR data represent the mean ± SEM of three independent experiments. $^{**}p < 0.005$, $^{***}p < 0.0001$, one-way ANOVA. Med, medium.

suggested in independent studies, we found a direct link for NOD2-responsive WNT signaling in the development of joint inflammations.

Further, RIP2/TAK1-independent activation of WNT signaling upon stimulation of NOD2 is another interesting observation made in the current study. Supporting our observation, RIP2-independent NOD2 functions were reported previously (38). In this study, we found that NOD2 interacted with LYPD6 to stimulate the WNT signaling cascade and induce activation of inflammasomes. Corresponding with the in vitro data, mice exhibiting acute arthritis upon MDP challenge displayed enhanced inflammasome activation. Interestingly, in line with the current observation, IL-1β and IL-18 produced via the activation of the NLRP3 inflammasome are known to drive the pathogenesis of osteoarthritis (39). Further, although the role for NOD2-induced inflammasome activation during the formation of active caspase-1 and the secretion of proinflammatory cytokine, such as IL-1β, was reported (14, 15), no reports of WNT-mediated activation of inflammasomes are known. Thus, these results underscore a novel inflammatory function of the WNT signaling cascade during joint inflammation and related inflammatory disorders.

NOD2-induced WNT signaling was found to regulate the expression of an E3 ubiquitin ligase, XIAP, to mediate the activation of inflammasomes. Different classes of IAPs—cytosolic IAP1, IAP2, and XIAP—were reported to assist the innate immune signaling responses, including those mediated by NOD2 (40, 41). Notably, IAPs also function to regulate inflammasome activation (42). However, the exact mechanism was not clear, because previous investigations suggested IAP-mediated positive (43) and negative (44) regulation of inflammasome activation. In the current study, we found that XIAP positively modulates NOD2-responsive NLRP3 inflammasome activation. Importantly, corresponding results were observed in the mice model of arthritis; inhibition of XIAP compromised the MDP-exacerbated acute arthritis phenotypes. Based on the previous reports underscoring the role for NLRP3 in NOD2 responses (17, 31) and arthritis (39) and the current observations, we propose that NOD2 signaling directs the expression of XIAP in macrophages that recruits to and activates NLRP3 inflammasomes to produce IL-1β and orchestrates acute arthritis in mice. Further, the exact function of XIAP in this context is still under investigation.

We demonstrated novel roles for WNT signaling–induced XIAP expression and subsequent inflammasome activation in NOD2-responsive development of acute arthritis in mice. These findings may aid in the better understanding of the pathogenesis of inflammatory arthritis and, thus, serve as potential therapeutic targets, as well as provide insights into the probable mechanisms of NOD2-orchestrated inflammatory disorders.

Acknowledgments

We thank the Central Animal Facility, Indian Institute of Science for providing mice for experimentation. We sincerely thank Dr. Derek W. Abbott for providing the NOD2 cDNA and RIP2 D/N constructs, Dr. Jonathan D. Ashwell for XIAP cDNA and XIAP D/N constructs, Dr. Gilbert Weidinger for spGFP-LYPD6 cDNA and spGFP-LYPD6 D/N constructs, Dr. Jun Nonomiya-Tsuji for TAK1 D/N constructs, Dr. Roel Nusse for TCF4 D/N construct, and Dr. Kumaravel Somasundaram for β-galactosidase reporter construct. We acknowledge Dr. Devram Sampat Ghorpade for critical comments and Dr. Sandeepa M. Eswarappa for help during the course of investigation.

Disclosures

The authors have no financial conflicts of interest.

References

1. Philpott, D. J., M. T. Sorbara, S. J. Robertson, K. Croitoru, and S. E. Girardin. 2014. NOD proteins: regulators of inflammation in health and disease. *Nat. Rev. Immunol.* 14: 9–23.
2. Kumagai, Y., and S. Akira. 2010. Identification and functions of pattern-recognition receptors. *J. Allergy Clin. Immunol.* 125: 985–992.
3. Chen, G., M. H. Shaw, Y. G. Kim, and G. Nuñez. 2009. NOD-like receptors: role in innate immunity and inflammatory disease. *Annu. Rev. Pathol.* 4: 365–398.
4. Hugot, J. P., M. Chamaillard, H. Zouali, S. Lesage, J. P. Cézard, J. Belaiche, S. Almer, C. Tysk, C. A. O'Morain, M. Gassull, et al. 2001. Association of NOD2 leucine-rich repeat variants with susceptibility to Crohn's disease. *Nature* 411: 599–603.
5. Ghorpade, D. S., A. Y. Sinha, S. Holla, V. Singh, and K. N. Balaji. 2013. NOD2-nitric oxide-responsive microRNA-146a activates Sonic hedgehog signaling to orchestrate inflammatory responses in murine model of inflammatory bowel disease. *J. Biol. Chem.* 288: 33037–33048.
6. Saha, S., J. Qi, S. Wang, M. Wang, X. Li, Y. G. Kim, G. Núñez, D. Gupta, and R. Dziarski. 2009. PGLYRP-2 and Nod2 are both required for peptidoglycan-induced arthritis and local inflammation. *Cell Host Microbe* 5: 137–150.
7. Rosenzweig, H. L., M. J. Jann, E. E. Vance, S. R. Planck, J. T. Rosenbaum, and M. P. Davey. 2010. Nucleotide-binding oligomerization domain 2 and Toll-like receptor 2 function independently in a murine model of arthritis triggered by intraarticular peptidoglycan. *Arthritis Rheum.* 62: 1051–1059.
8. Rosenzweig, H. L., M. M. Jann, T. T. Glant, T. M. Martin, S. R. Planck, W. van Eden, P. J. van Kooten, R. A. Flavell, K. S. Kobayashi, J. T. Rosenbaum, and M. P. Davey. 2009. Activation of nucleotide oligomerization domain 2 exacerbates a murine model of proteoglycan-induced arthritis. *J. Leukoc. Biol.* 85: 711–718.
9. Miceli-Richard, C., S. Lesage, M. Rybojad, A. M. Prieur, S. Manouvrier-Hanu, R. Häfner, M. Chamaillard, H. Zouali, G. Thomas, and J. P. Hugot. 2001. CARD15 mutations in Blau syndrome. *Nat. Genet.* 29: 19–20.
10. Shirtliff, M. E., and J. T. Mader. 2002. Acute septic arthritis. *Clin. Microbiol. Rev.* 15: 527–544.
11. Joosten, L. A., B. Heinhuis, S. Abdollahi-Roodsaz, G. Ferwerda, L. Lebourhis, D. J. Philpott, M. A. Nahori, C. Popa, S. A. Morre, J. W. van der Meer, et al. 2008. Differential function of the NACHT-LRR (NLR) members Nod1 and Nod2 in arthritis. *Proc. Natl. Acad. Sci. USA* 105: 9017–9022.
12. van der Heijden, I. M., B. Wilbrink, I. Tchetverikov, I. A. Schrijver, L. M. Schouls, M. P. Hazenberg, F. C. Breedveld, and P. P. Tak. 2000. Presence of bacterial DNA and bacterial peptidoglycans in joints of patients with rheumatoid arthritis and other arthritides. *Arthritis Rheum.* 43: 593–598.
13. Strober, W., P. J. Murray, A. Kitani, and T. Watanabe. 2006. Signalling pathways and molecular interactions of NOD1 and NOD2. *Nat. Rev. Immunol.* 6: 9–20.
14. Tschopp, J., F. Martinon, and K. Burns. 2003. NALPs: a novel protein family involved in inflammation. *Nat. Rev. Mol. Cell Biol.* 4: 95–104.
15. Stutz, A., D. T. Golenbock, and E. Latz. 2009. Inflammasomes: too big to miss. *J. Clin. Invest.* 119: 3502–3511.
16. Rathinam, V. A., S. K. Vanaja, and K. A. Fitzgerald. 2012. Regulation of inflammasome signaling. *Nat. Immunol.* 13: 333–342.
17. Martinon, F., K. Burns, and J. Tschopp. 2002. The inflammasome: a molecular platform triggering activation of inflammatory caspases and processing of proIL-beta. *Mol. Cell* 10: 417–426.
18. Bansal, K., and K. N. Balaji. 2011. Intracellular pathogen sensor NOD2 programs macrophages to trigger Notch1 activation. *J. Biol. Chem.* 286: 5823–5835.
19. Moreira, L. O., and D. S. Zamboni. 2012. NOD1 and NOD2 Signaling in Infection and Inflammation. *Front. Immunol.* 3: 328.
20. Koslowski, M. J., Z. Teltschik, J. Beisner, E. Schaeffeler, G. Wang, I. Kübler, M. Gersemann, R. Cooney, D. Jewell, W. Reinisch, et al. 2012. Association of a functional variant in the Wnt co-receptor LRP6 with early onset ileal Crohn's disease. *PLoS Genet.* 8: e1002523.
21. Koslowski, M. J., I. Kübler, M. Chamaillard, E. Schaeffeler, W. Reinisch, G. Wang, J. Beisner, A. Teml, L. Peyrin-Biroulet, S. Winter, et al. 2009. Genetic variants of Wnt transcription factor TCF-4 (TCF7L2) putative promoter region are associated with small intestinal Crohn's disease. *PLoS ONE* 4: e4496.
22. Wehkamp, J., G. Wang, I. Kübler, S. Nuding, A. Gregorieff, A. Schnabel, R. J. Kays, K. Fellermann, O. Burk, M. Schwab, et al. 2007. The Paneth cell alpha-defensin deficiency of ileal Crohn's disease is linked to Wnt/Tcf-4. *J. Immunol.* 179: 3109–3118.
23. Sen, M. 2005. Wnt signalling in rheumatoid arthritis. *Rheumatology (Oxford)* 44: 708–713.
24. Miao, C. G., Y. Y. Yang, X. He, X. F. Li, C. Huang, Y. Huang, L. Zhang, X. W. Lv, Y. Jin, and J. Li. 2013. Wnt signaling pathway in rheumatoid arthritis, with special emphasis on the different roles in synovial inflammation and bone remodeling. *Cell. Signal.* 25: 2069–2078.
25. Rabelo, Fde. S., L. M. da Mota, R. A. Lima, F. A. Lima, G. B. Barra, J. F. de Carvalho, and A. A. Amato. 2010. The Wnt signaling pathway and rheumatoid arthritis. *Autoimmun. Rev.* 9: 207–210.
26. Futami, I., M. Ishijima, H. Kaneko, K. Tsuji, N. Ichikawa-Tomikawa, R. Sadatsuki, T. Muneta, E. Arikawa-Hirasawa, I. Sekiya, and K. Kaneko. 2012. Isolation and characterization of multipotential mesenchymal cells from the mouse synovium. *PLoS ONE* 7: e45517.
27. Özhan, G., E. Sezgin, D. Wehner, A. S. Pfister, S. J. Kühl, B. Kagermeier-Schenk, M. Kühl, P. Schwille, and G. Weidinger. 2013. Lypd6 enhances Wnt/β-catenin signaling by promoting Lrp6 phosphorylation in raft plasma membrane domains. *Dev. Cell* 26: 331–345.
28. Zhang, Y., Q. Lang, J. Li, F. Xie, B. Wan, and L. Yu. 2010. Identification and characterization of human LYPD6, a new member of the Ly-6 superfamily. *Mol. Biol. Rep.* 37: 2055–2062.

29. Barnich, N., J. E. Aguirre, H. C. Reinecker, R. Xavier, and D. K. Podolsky. 2005. Membrane recruitment of NOD2 in intestinal epithelial cells is essential for nuclear factor-kappaB activation in muramyl dipeptide recognition. *J. Cell Biol.* 170: 21–26.
30. Lécine, P., S. Esmiol, J. Y. Métais, C. Nicoletti, C. Nourry, C. McDonald, G. Nunez, J. P. Hugot, J. P. Borg, and V. Ollendorff. 2007. The NOD2-RICK complex signals from the plasma membrane. *J. Biol. Chem.* 282: 15197–15207.
31. Martinon, F., L. Agostini, E. Meylan, and J. Tschopp. 2004. Identification of bacterial muramyl dipeptide as activator of the NALP3/cryopyrin inflammasome. *Curr. Biol.* 14: 1929–1934.
32. Wang, X. H., X. Sun, X. W. Meng, Z. W. Lv, Y. J. Du, Y. Zhu, J. Chen, D. X. Kong, and S. Z. Jin. 2010. beta-catenin siRNA regulation of apoptosis- and angiogenesis-related gene expression in hepatocellular carcinoma cells: potential uses for gene therapy. *Oncol. Rep.* 24: 1093–1099.
33. Zhang, F., A. Chen, J. Chen, T. Yu, and F. Guo. 2011. SiRNA-mediated silencing of beta-catenin suppresses invasion and chemosensitivity to doxorubicin in MG-63 osteosarcoma cells. *Asian Pac. J. Cancer Prev.* 12: 239–245.
34. Bauler, L. D., C. S. Duckett, and M. X. O'Riordan. 2008. XIAP regulates cytosol-specific innate immunity to *Listeria* infection. *PLoS Pathog.* 4: e1000142.
35. Ospelt, C., F. Brentano, A. Jüngel, Y. Rengel, C. Kolling, B. A. Michel, R. E. Gay, and S. Gay. 2009. Expression, regulation, and signaling of the pattern-recognition receptor nucleotide-binding oligomerization domain 2 in rheumatoid arthritis synovial fibroblasts. *Arthritis Rheum.* 60: 355–363.
36. Ma, Y., and R. M. Pope. 2005. The role of macrophages in rheumatoid arthritis. *Curr. Pharm. Des.* 11: 569–580.
37. Strober, W., and T. Watanabe. 2011. NOD2, an intracellular innate immune sensor involved in host defense and Crohn's disease. *Mucosal Immunol.* 4: 484–495.
38. Travassos, L. H., L. A. Carneiro, M. Ramjeet, S. Hussey, Y. G. Kim, J. G. Magalhães, L. Yuan, F. Soares, E. Chea, L. Le Bourhis, et al. 2010. Nod1 and Nod2 direct autophagy by recruiting ATG16L1 to the plasma membrane at the site of bacterial entry. *Nat. Immunol.* 11: 55–62.
39. Jin, C., P. Frayssinet, R. Pelker, D. Cwirka, B. Hu, A. Vignery, S. C. Eisenbarth, and R. A. Flavell. 2011. NLRP3 inflammasome plays a critical role in the pathogenesis of hydroxyapatite-associated arthropathy. *Proc. Natl. Acad. Sci. USA* 108: 14867–14872.
40. Bertrand, M. J., K. Doiron, K. Labbé, R. G. Korneluk, P. A. Barker, and M. Saleh. 2009. Cellular inhibitors of apoptosis cIAP1 and cIAP2 are required for innate immunity signaling by the pattern recognition receptors NOD1 and NOD2. *Immunity* 30: 789–801.
41. Krieg, A., R. G. Correa, J. B. Garrison, G. Le Negrate, K. Welsh, Z. Huang, W. T. Knoefel, and J. C. Reed. 2009. XIAP mediates NOD signaling via interaction with RIP2. *Proc. Natl. Acad. Sci. USA* 106: 14524–14529.
42. Vandenabeele, P., and M. J. Bertrand. 2012. The role of the IAP E3 ubiquitin ligases in regulating pattern-recognition receptor signalling. *Nat. Rev. Immunol.* 12: 833–844.
43. Labbé, K., C. R. McIntire, K. Doiron, P. M. Leblanc, and M. Saleh. 2011. Cellular inhibitors of apoptosis proteins cIAP1 and cIAP2 are required for efficient caspase-1 activation by the inflammasome. *Immunity* 35: 897–907.
44. Vince, J. E., W. W. Wong, I. Gentle, K. E. Lawlor, R. Allam, L. O'Reilly, K. Mason, O. Gross, S. Ma, G. Guarda, et al. 2012. Inhibitor of apoptosis proteins limit RIP3 kinase-dependent interleukin-1 activation. *Immunity* 36: 215–227.